Diclofenac Adsorption from Contaminated Water onto Olive-Leaf-Derived Adsorbent

***Zuhier Alakayleh*[1*]**

[1] Civil and Environmental Engineering Department, College of Engineering, Mutah University, Al-Karak, Jordan.

ABSTRACT

This study investigates the adsorption of diclofenac (DCF) onto an olive leaf-derived adsorbent. The harvested olive leaves were washed, dried, and powdered then extracted with 80% ethanol. The extraction was filtered, washed with sodium hypochlorite, and ethanol, and then dried. The material was then activated using sodium hydroxide, phosphoric acid, and dead sea water, for the adsorption of DCF from contaminated water being investigated. Various operational parameters such as dosage, contact time, DCF concentration, and pH were systematically varied to understand their influence on adsorption efficiency. The kinetics of DCF adsorption followed pseudo-second-order kinetics. Isothermal studies revealed that the adsorption process conforms well with the Freundlich isotherm, suggesting multilayer adsorption onto a heterogeneous surface. Thermodynamic analysis indicated that the adsorption process is spontaneous and exothermic. Morphological analysis completed using the SEM data demonstrated a transformation in the porous structure of the adsorbent, indicating effective pore occupation by DCF molecules post-adsorption. Overall, the results demonstrate the effectiveness of olive leaf-derived adsorbent in efficiently removing DCF from aqueous solutions.

Keywords: Contamination; Emerging Contaminant; Thermodynamics; Water Treatment; Adsorption.

1. INTRODUCTION

Pollution of water by pharmaceutical chemicals has been a major environmental concern in recent years [1]. One of the widely used pharmaceutical medications of interest is diclofenac (DCF), the most-selling nonsteroidal drug known for its pain-relieving and anti-inflammatory properties [2, 3]. Many studies including [4] and [5] have found DCF in water bodies. [6] found DCF in 83% of European rivers' water samples. [7] detected DCF in China's Huangpu and Beiyun rivers. In Taiwanese waterways, [8] found DCF in 23 different sites. Several studies have also found DCF in water bodies in USA, Korea, Spain, Serbia, Greece, and Portugal, as reported by [9-15].

[*]***Corresponding author: Zuhier Alakayleh***
zalakayleh@mutah.edu.jo
Received: 13/05/2024 Accepted: 18/07/2024.
DOI: https://doi.org/10.35516/jjps.v18i1.2644

The presence of DCF in water can be toxic to both humans and several aquatic organisms, including bacteria, algae, fish, and microcrustaceans [16, 17]. DCF's presence in many water bodies across the world can be related to its widespread use as a painkiller and anti-inflammatory medicine and its resistance to degradation using typical treatment conditions. Only about 60% of DCF can be eliminated from water using traditional treatment methods[18-20].

Currently, there is a need to develop more advanced and effective technologies to remove DCF from water systems. Some promising methods include ozonation[21], membrane filtration[22], advanced oxidation techniques [23], Fenton oxidation[24], and adsorption[25]. Several of the aforementioned methods often come with various complications including intricate procedures, high expenses, and the management of toxic sludge[26]. However,

adsorption remains a favored choice due to its simplicity, efficiency, and cost-effectiveness [26, 27].

Many materials are available for DCF adsorption from contaminated water including chemically activated cocoa pod husks[28], activated carbon derived from sewage sludge[29], graphene oxide[30], multiwalled carbon nanotubes[31], commercial organoclay[32], and activated carbon from tea waste[33].

Jordan is one of the main olive producing countries in the world and harvests approximately 296,814 tons of olives every year [34]. In the harvesting season, significant volumes of leaves are generated as waste. [35] introduced an adsorbent derived from olive leaves for capturing lead, a highly toxic heavy metal, from polluted water. The objective of this study is to investigate the efficacy of the olive-leaf-derived adsorbent for removing DCF from contaminated water. The effect of several adsorption parameters such as adsorbent dosage, contact time, initial DCF concentration, solution pH, and temperature were investigated. The experimental data are used to develop an equilibrium isotherm and also a kinetic model for predicting the adsorption process.

2. MATERIALS AND METHODS

2.1. Materials

During the olive harvesting season in 2022, fresh olive tree leaves were gathered from a farm located in Irbid, Jordan. Dead Sea water was brought from the Dead Sea, Jordan. The diclofenac (DCF) used in the study was obtained from Dar Al-Dawa Industrial Company, Amman-Jordan. Pure sodium hydroxide pellets (with a purity of 98.5%) were procured from Fisher Scientific International, UK. Jordan Chemical Industries supplied the sodium hypochlorite. Sigma Aldrich supplied acetonitrile with a purity of 99.9%. Jordan Phosphate Mines Company provided the phosphoric acid.

2.2. Preparation of the olive-leaf-derived adsorbent

Freshly harvested olive leaves underwent thorough washing with distilled water to remove stuck dirt, followed by controlled air-drying in a dark condition. The dried leaves were then finely powdered using a grinder and subjected to extraction following the procedure detailed by [36]. The procedure encompassed combining 200 g of powdered leaves with 500 mL of 80% ethanol extraction solvent in a volumetric flask, followed by 5 hours of agitation to facilitate efficient extraction of plant constituents. The extracted material was kept in the room until reaching lab temperature and then filtered using a Whatman No.42 filter in order to obtain fine particles only. Soaking the fine sample with 5 L of sodium hypochlorite and filtering resulted in a white creamy fine sample (the process was repeated about fives times). The white creamy sample was cleaned from the sodium hypochlorite when it was washed with 80% ethanol and distilled water. The clean sample was dried in an oven at 70°C. The obtained dry sample was activated following the procedure introduce by [37] and [35]. The method involves combining 10 g of the sample with 3.5 g sodium hydroxide and 2 mL phosphoric acid along with progressively adding 10 mL of Dead Sea water with stirring for 15 minutes. The obtained product was then cleaned with distilled water and dried in an oven at 70°C. The applicability of using the obtained dry material in the adsorption of DCF from contaminated water was investigated in this study.

The abundance of valuable salts in Dead Sea water is crucial in the activation method to enhance the adsorption capacity. Where the active binding sites in the biomass are transformed from H+ to Ca+, Na+, Mg+, and K+ with the help from using phosphoric acid and sodium hydroxide [35, 37].

2.3. Experimental studies

The Phenom XL G2 SEM was used to study the surface structure of the olive-leaf-based adsorbent. SEM was performed in high vacuum with a 15 kV accelerating voltage to improve image quality. The samples were conductive carbon taped on SEM stubs and platinum-sputter-coated before imaging. Samples were mounted on SEM stubs with conductive carbon tape and sputter-coated with platinum before imaging. This preparation increased

electrical conductivity and reduced imaging charging.

All adsorption studies used 10 mL DCF-contaminated solutions. Testing samples were placed in a temperature-controlled water shaker bath at 100 rpm. After treatment, DCF concentrations were determined using Thermo-Electron Corporation HPLC at 280 nm and 1 mL/min.

Several experiments were conducted to determine how various operational parameters affect DCF adsorption. To study how the operational parameters affect absorptiometry, the adsorbent dose (5–80 mg/mL), initial DCF concentration (0.04–1 mg/mL), contact time (5–120 minutes), and solution pH (6–11 pH) were varied systematically. DFC removal percentages were estimated using Equation 1 presented in Table 1. Where C_i and C_f are DCF concentrations at the beginning (initial) and end (final) of the adsorption (mg/mL), respectively.

Table 1. Adsorption removal percentage, capacity, isotherms, and kinetics governing equations utilized in this study

Equation*	Reference	Equation sequence
$\%\ DCF\ removal = (C_i - C_f)/C_i \times 100\%$	[38]	(1)
$C_e/q_e = 1/q_{max}b + C_e/q_{max}$	[39]	(2)
$log\ q_e = logK_f + (1/n)\ logC_e$	[40]	(3)
$q_e = \left[(C_i - C_f)V\right]/M$	[35]	(4)
$log\ (q_e - q_t) = logq_e + (K_1/2.303)\ t$	[41]	(5)
$t/q_t = 1/(K_2 q_e^2) + (1/q_e)\ t$	[42]	(6)
$q_t = [(C_i - C_t)V]/M$	[28]	(7)
$K_L = q_e/C_e$	[43]	(8)
$\Delta G^o = -RT \ln K_L$	[44]	(9)
$\ln K_L = (\Delta S^o/R) - (\Delta H^o/(RT))$	[45]	(10)

* The symbols in Table 1 are all defined in the text at their first occurrence.

The adsorption isotherm was investigated by conducting experimental tests y varying C_i (from 0.04 to 1 mg/mL) while ensuring the attainment of the equilibrium condition with constant values for the remaining parameters. The obtained equilibrium data were subjected to fitting using the two commonly employed models, Langmuir (Equation 2 in Table 1) and Freundlich (Equation 3 in Table 1) isotherms. Where q_e is the adsorption capacity at equilibrium (mg/g) which can be calculated using Equation 4, q_{max} is the maximum adsorption capacity (mg/g), b is the Langmuir constant (L/mg), K_f is the Freundlich constant that represents the measure of the adsorption capacity ((mg/g) $(L/mg)^n$), n represents the adsorption intensity parameter, V is the volume of the solution (mL), and M is the mass of the olive-leaf-derived adsorbent (g).

The kinetics of DCF adsorption onto the olive leaf-derived adsorbent were investigated using pseudo-first-order (Equation 5 in Table 1) and pseudo-second-order (Equation 6 in Table 1) kinetics models. Where K_1 and K_2 are the adsorption rate constant for pseudo-first-order and pseudo-second-order kinetic models, respectively, q_t is the adsorption capacity at time t which can be estimated using Equation 7 (Table 1).

Thermodynamic parameters for the adsorption of DCF onto the olive leaf-derived adsorbent were determined through experimental tests conducted at different temperatures (from 25 to 45 ºC), while keeping all other parameters constant. These thermodynamic parameters encompass the Gibbs free energy change (ΔG^o), the enthalpy change (ΔH^o), and the entropy change (ΔS^o), providing valuable insights into the adsorption process.

Equation 8-10 (Table 1) were used to estimate the thermodynamic parameters. Where K_L is the equilibrium adsorption constant, R is universal gas constant, and T is the temperature (in Kelvin).

3. RESULTS AND DISCUSSION

3.1. Scanning electron microscopic analysis

The morphology of the olive leaf-derived adsorbent reveals a highly porous structure (Figure 1A). The SEM images of the olive leaf-derived adsorbent depict a notable transformation from a porous structure before DCF adsorption (Figure 1A) to a seemingly filled appearance post-adsorption (Figure 1B), indicating significant pore occupation by DCF molecules. This observation suggests a robust adsorption mechanism where DCF molecules effectively penetrated the pore structure of the adsorbent to occupy available surface sites.

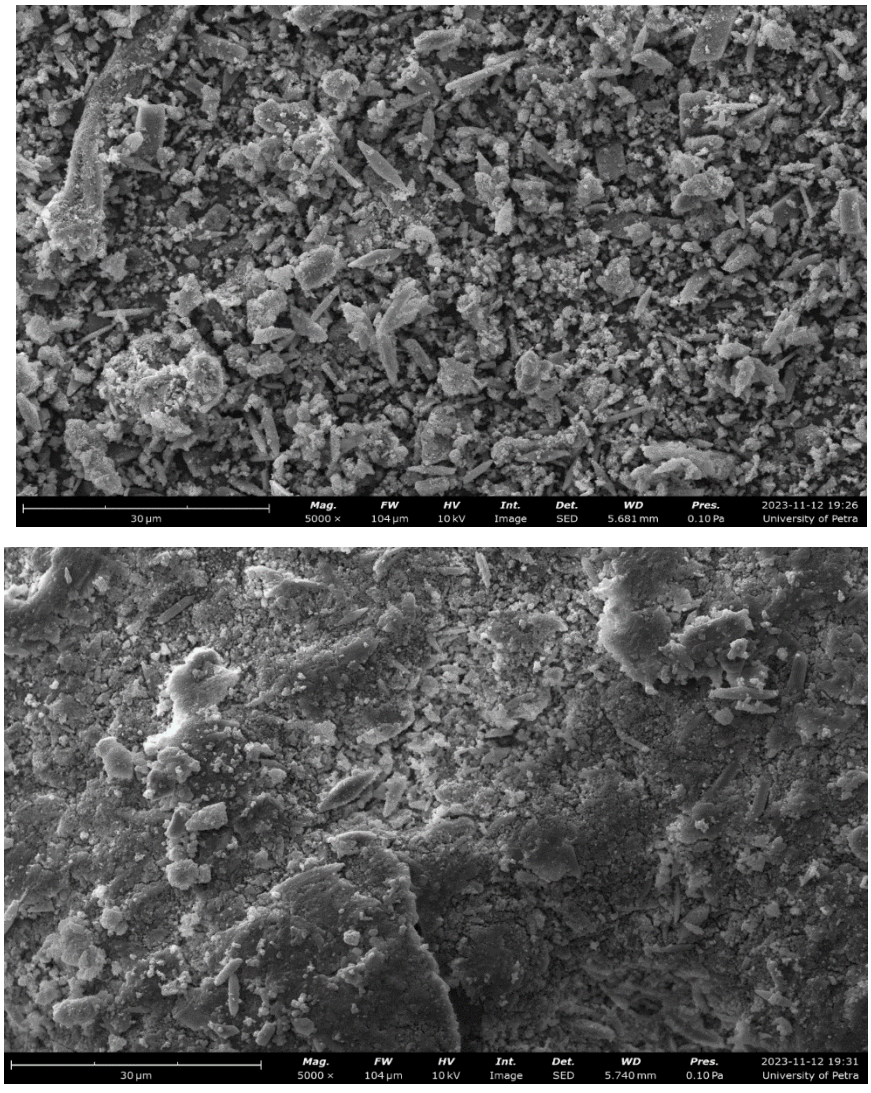

Figure 1. SEM images of the olive-leaf-derived adsorbent (A) before adsorption and (B) after adsorption

3.2. Effect of adsorbent dose

The adsorption of DCF (concentration = 1 mg/mL) was performed using the olive-leaf-derived adsorbent across a range of doses (5 to 80 mg/mL) over 120 minutes at a pH of 6. Initially, at 5 mg/mL, DCF removal was only around 8%, whereas at 80 mg/mL, it dramatically increased to 89% (Figure 2). This notable improvement in removal percentage with higher doses can be attributed to the increased availability of active sites on the adsorbent surface [46].

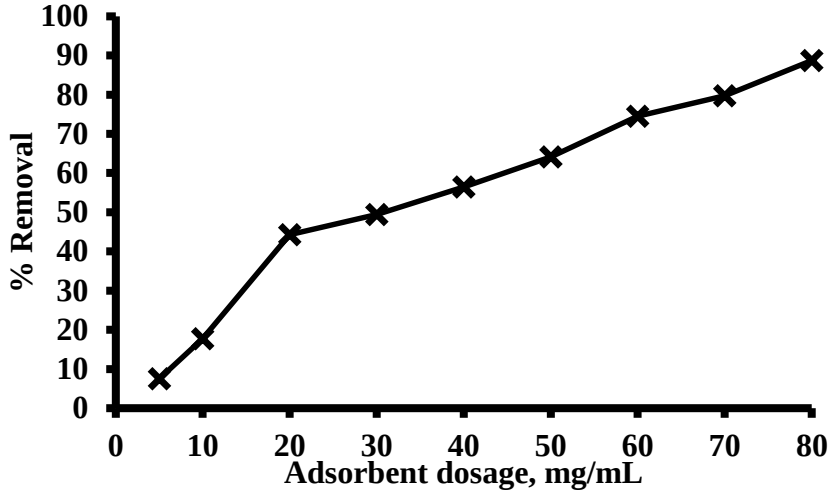

Figure 2. Effect of the olive-leaf-derived adsorbent dosage on DCF adsorption removal percentage

3.3. Effect of contact time

To establish the equilibrium time required for DCF adsorption (initial concentration = 1 mg/mL), experiments were conducted over a time range of 5 to 120 minutes, using a constant adsorbent dosage of 80 mg/mL. Figure 3 depicts the observed trend, showing a steady increase in uptake with time until equilibrium was reached at 60 minutes. Notably, no further uptake was recorded beyond this duration. The decline in adsorption over time can be attributed to the depletion of available adsorption sites [47].

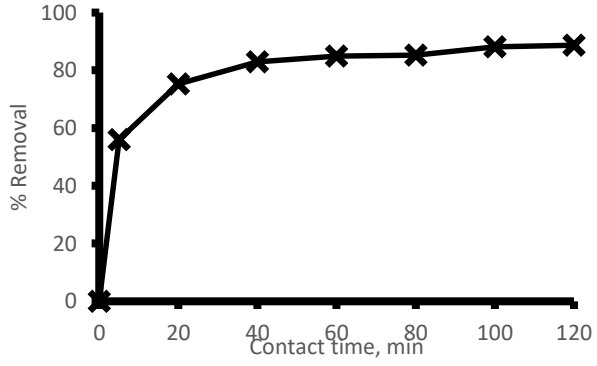

Figure 3. Effect of contact time on DCF adsorption removal percentage onto the olive-leaf-derived adsorbent

3.4. Effect of solution pH

The experimental findings presented in Figure 4 demonstrated the highest removal percentage of DCF at pH 6, reaching approximately 88.7%. As the pH increased from 7 to 11, there was a slight decrease in the removal percentage, although remaining relatively high (stabilizing around 83%). This trend suggests that within the tested pH range (6 to 11), the adsorption of DCF onto the olive leaf-derived adsorbent is consistently effective, with slightly enhanced efficiency observed at lower pH values. The pH levels below 6 were not examined because DCF is only slightly soluble in water under acidic conditions [48].

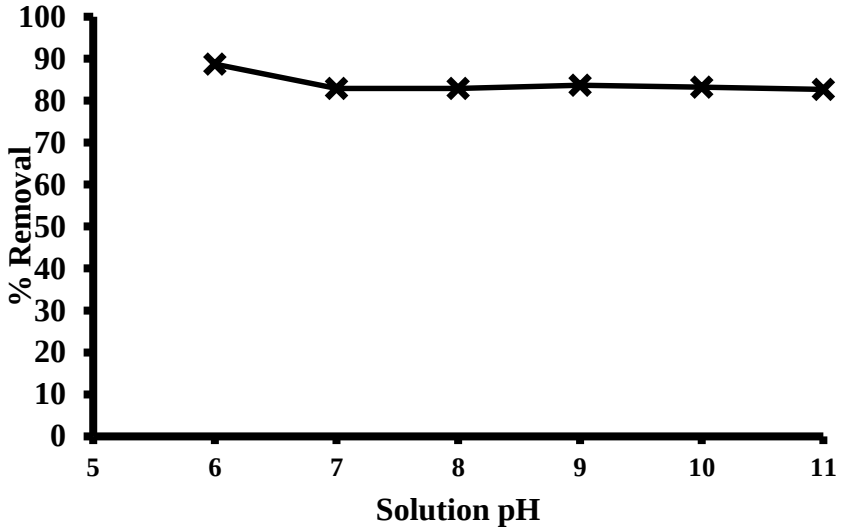

Figure 4. Effect of Solution pH on the percentage of DCF adsorption removal using olive leavf-derived adsorbent (Adsorbent dose = 80 mg/mL; contact time = 120 min)

Effect of DCF initial concentration

Figure 5 presents the outcomes of an experimental investigation aimed at evaluating the influence of varying initial concentrations of DCF (0.04 to 1 mg/L) on its removal efficiency using the olive-leaf-derived adsorbent. As initial DCF levels increased, removal percentages declined. The peaked removal percentage of 88.7% was obtained at an initial concentration of 0.04 mg/mL, which was decreased to 68.41% at 1 mg/mL. The increase in DCF concentration reduces the available adsorption sites, which may explain the decline in removal percentages [33, 49, 50].

3.5. Adsorption kinetics

The investigation of the adsorption kinetics data was carried out using the pseudo-first-order and pseudo-second-order models. The linearized forms of these two models were used, which are presented in Equations 5 and 6 in Table 1. Results presented in Figure 6 show that both models represent the kinetics data of DCF adsorption onto the olive-leaf-derived adsorbent well. A summary of both models' parameters are presented in Table 2. For the pseudo-first-order model, the computed equilibrium adsorption capacity (q_e) and rate constant (K_1) were 6.03 mg/g and 3.7×10^{-2} 1/min, respectively, and the estimated R^2 value was 92.2 %, indicating a good correlation with the experimental data. Conversely, the pseudo-second-order model showed a lower q_e of 0.456 mg/g, a rate constant (K_2) of 0.591 g/(mg.min), and an excellent match to the experimental data (R^2 = 99.9 %). The higher R^2 value of the pseudo-second-order model indicates a more accurate representation of the adsorption kinetics.

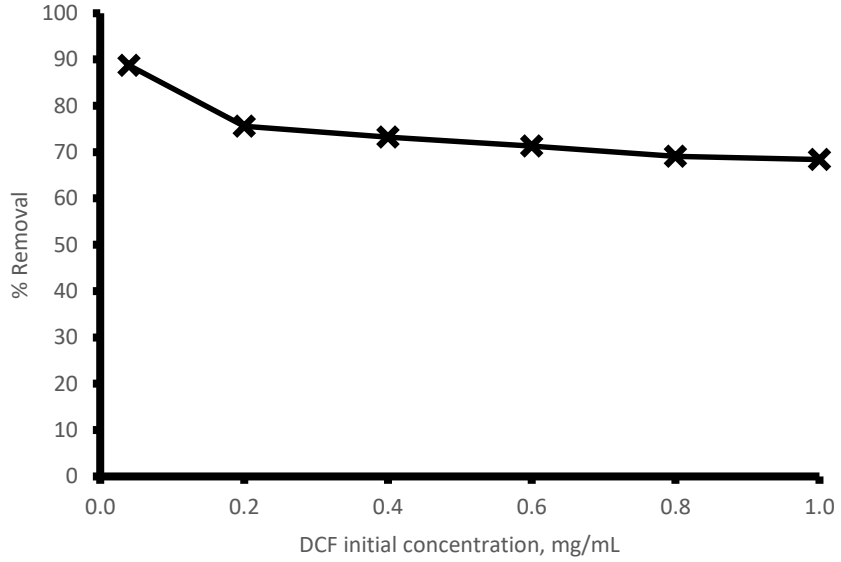

Figure 5. Effect of initial DCF concentration on the percentage of DCF adsorption removal by olive leaf-derived adsorbent

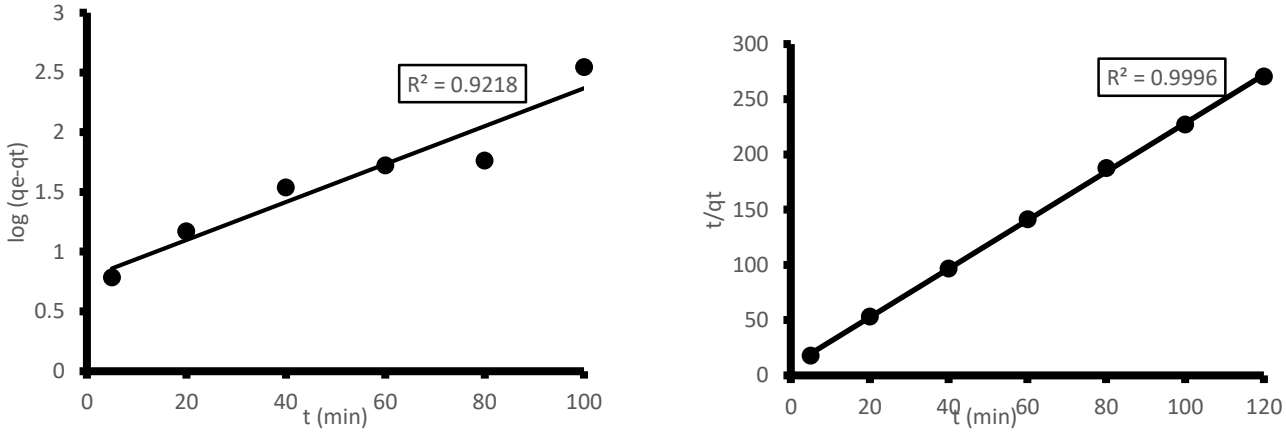

A **B**

Figure 6. Fitting of adsorption kinetic data for DCF adsorption onto the olive leaves-derived adsorbent using: (A) pseudo-first-order and (B) pseudo-second-order

Table 2. Kinetic parameters for DCF adsorption onto olive-leaf-derived adsorbent

Kinetics parameters and R^2	
pseudo-first-order model	
q_e (mg/g)	6.03
K_1 (1/min)	3.7×10^{-2}
R^2	92.2%
pseudo-second-order model	
q_e (mg/g)	0.456
K_2 (g/(mg.min))	0.591
R^2	99.9%

3.6. Adsorption isotherms

The fittings of the isotherm experimental data were compared against both Langmuir and Freundlich models. The Freundlich model goodness of fit (R^2 = 99.5%) demonstrated superior fitting compared to the Langmuir model (R^2 = 76.1 %). Figure 7 demonstrates that the Freundlich isotherm offers a more precise depiction of the experimental data.

The Freundlich isotherm, defined by the maximum adsorption capacity (Q_{max}) and the Langmuir constant (K_L), models monolayer adsorption on homogeneous surfaces [51, 52]. As reported in Table 3, the Langmuir constant K_L was found to be 0.00408 and the maximum adsorption capacity Q_{max} was found to be 14 mg/g. The low R^2 value of (76%) suggests that there are deviations from monolayer adsorption or surface homogeneity. Lower R^2 values prompted inquiries regarding the suitability of the Langmuir model in completely elucidating the adsorption of DCF on the adsorbent derived from olive leaves.

The Freundlich isotherm, defined by the Freundlich constant (K_f) and the exponent (n), models multilayer adsorption on heterogeneous surfaces [35, 43, 53]. The high R^2 value of 99.5% suggests a robust correlation with the experimental data. The Freundlich exponent (n) of 1.434 suggests favorable adsorption, as values between 1 and 10 typically indicate good adsorption [54]. The Freundlich constant (K_f) of 0.1449 represents the adsorption capacity (Table 3).

In summary, the Freundlich isotherm model appears to be more appropriate for describing the adsorption of DCF onto the olive-leaf-derived adsorbent, indicating multilayer, heterogeneous adsorption under favorable conditions.

3.7. Thermodynamic parameters

The plot of ln (K_L) versus 1/T (Figure 8) shows a linear relationship, suggesting that the adsorption process follows the Van't Hoff equation. The slope and intercept from Figure 8 were used to calculate the values of the enthalpy (ΔH^o) and entropy (ΔS^o). The obtained negative values for both ΔH^o and ΔS^o (Table 4) indicated that the adsorption process of DCF onto the olive-leaf-derived adsorbent is exothermic and associated with a decrease in randomness. The calculated Gibbs free energy (ΔG^o) values (Table 4) were also negative at all temperatures, indicating that the adsorption process is thermodynamically favorable and spontaneous [55].

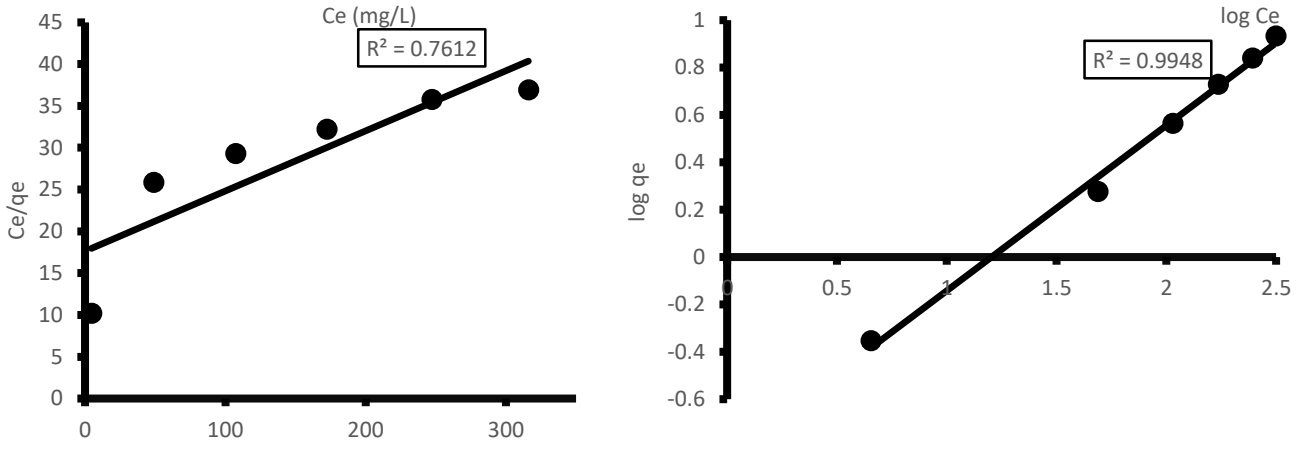

A **B**

Figure 7. Fitting of equilibrium data for DCF adsorption onto the olive leaf-derived adsorbent to the isotherm models. (A) Langmuir isotherm and (B) Freundlich isotherm

Table 3. Isotherm parameters for DCF adsorption onto olive-leaf-derived adsorbent

Isotherm models	isotherm parameters and regression coefficients	
	Q_m (mg/g)	14
Langmuir isotherm	K_L (L/mg)	0.00408
	R^2	76.1%
	K_f (mg/g).(L/mg)^n	0.1449
Freundlich isotherm	n	1.434
	R^2	99.5%

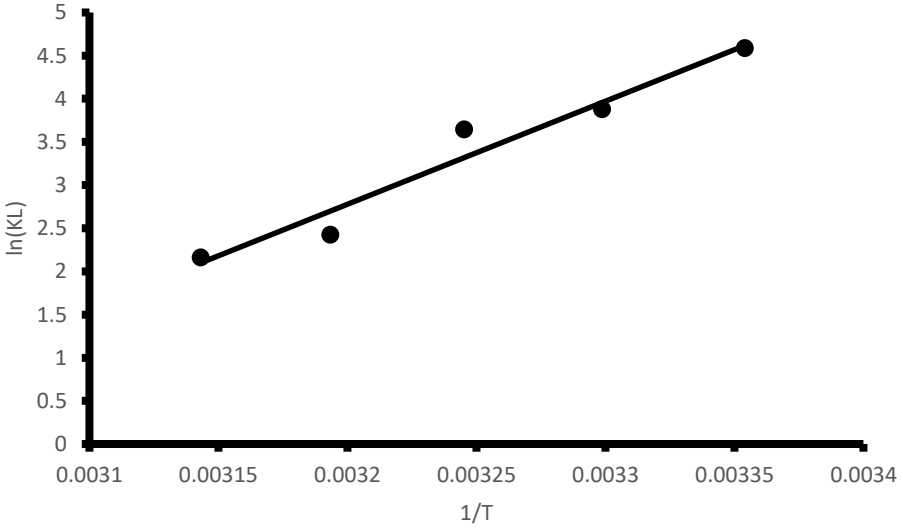

Figure 8. The plot of ln (K_L) versus 1/T for determining thermodynamic parameters of DCF adsorption on the olive-leaf-derived adsorbent

Table 4. Thermodynamic parameters for the adsorption of DCF onto the olive-leaf-derived adsorbent.

ΔH^o (kJ/mol)	ΔS^o (J/mol.K)	ΔG^o (kJ/mol)				
		Temperature (K)				
		298	303	308	313	318
-99.299	-0.295	-11.37	-9.77	-9.34	-6.32	-5.72

4. CONCLUSIONS

Our investigation examined the adsorption behavior of diclofenac (DCF) onto olive leaf-derived adsorbent. We explored the influence of adsorbent dosage, contact time, initial DCF concentration, and pH on adsorption efficiency. Our data show that 80 mg/mL adsorbent dose, 120 min contact time, and 0.04 mg/L DCF initial concentration are the optimal conditions for maximum removal. Kinetic studies demonstrated rapid uptake, which was well represented by pseudo-second-order model. The isotherm analysis highlighted Freundlich isotherm is the best option for describing the sorption reaction. The results of the thermodynamic analyses confirmed the spontaneous, exothermic nature of the sorption process. The study shows olive-leaf-derived absorbents can be extremely useful for treating DCF-contaminated water. Future research might be interesting to focus on developing pilot tests to evaluate the feasibility and cost-effectiveness in large-scale applications.

REFERENCES

1. Beltrán F.J., Pocostales P., Álvarez P.M., López-Piñeiro F. Catalysts to improve the abatement of sulfamethoxazole and the resulting organic carbon in water during ozonation. *Appl. Catal. B Environ.* 2009; 92(3-4):262–270.
2. Silveira C., Shimabuku-Biadola Q.L., Silva M.F., Vieira M.F., Bergamasco R. Development of an activated carbon impregnation process with iron oxide nanoparticles by green synthesis for diclofenac adsorption. *Environ. Sci. Pollut. Res.* 2020; 27:6088–6102.
3. Al-Zaubai N.M.S., Al-Anbari H.G., Alsaady A.A.H. The efficacy and tolerability of the use of combined versus single analgesic and prophylactic medications in severe migraine. *Jordan J. Pharm. Sci.* 2023; 16(2).
4. Schwaiger J., Ferling H., Mallow U., Wintermayr H., Negele R. Toxic effects of the non-steroidal anti-inflammatory drug diclofenac: Part I: histopathological alterations and bioaccumulation in rainbow trout. *Aquat. Toxicol.* 2004; 68(2):141–150.
5. Sotelo J.L., Ovejero G., Rodríguez A., Álvarez S., Galán J., García J. Competitive adsorption studies of caffeine and diclofenac aqueous solutions by activated carbon. *Chem. Eng. J.* 2014; 240:443–453.
6. Loos R., Gawlik B.M., Locoro G., Rimaviciute E., Contini S., Bidoglio G. EU-wide survey of polar organic persistent pollutants in European river waters. *Environ. Pollut.* 2009; 157(2):561–568.
7. Dai G., Wang B., Huang J., Dong R., Deng S., Yu G. Occurrence and source apportionment of pharmaceuticals and personal care products in the Beiyun River of Beijing, China. *Chemosphere.* 2015; 119:1033–1039.
8. Lin A.Y.-C., Yu T.-H., Lin C.-F. Pharmaceutical contamination in residential, industrial, and agricultural waste streams: risk to aqueous environments in Taiwan. *Chemosphere.* 2008; 74(1):131–141.
9. Benotti M.J., Trenholm R.A., Vanderford B.J., Holady J.C., Stanford B.D., Snyder S.A. Pharmaceuticals and endocrine disrupting compounds in US drinking water. *Environ. Sci. Technol.* 2009; 43(3):597–603.

10. Behera S.K., Kim H.W., Oh J.-E., Park H.-S. Occurrence and removal of antibiotics, hormones and several other pharmaceuticals in wastewater treatment plants of the largest industrial city of Korea. *Sci. Total Environ.* 2011; 409(20):4351–4360.
11. Camacho-Muñoz D., Martín J., Santos J.L., Aparicio I., Alonso E. Concentration evolution of pharmaceutically active compounds in raw urban and industrial wastewater. *Chemosphere.* 2014; 111:70–79.
12. Camacho-Muñoz M., Santos J., Aparicio I., Alonso E. Presence of pharmaceutically active compounds in Donana Park (Spain) main watersheds. *J. Hazard. Mater*. 2010; 177(1-3):1159–1162.
13. Petrović M., Škrbić B., Živančev J., Ferrando-Climent L., Barcelo D. Determination of 81 pharmaceutical drugs by high performance liquid chromatography coupled to mass spectrometry with hybrid triple quadrupole–linear ion trap in different types of water in Serbia. *Sci. Total Environ.* 2014; 468:415–428.
14. Kosma C.I., Lambropoulou D.A., Albanis T.A. Investigation of PPCPs in wastewater treatment plants in Greece: occurrence, removal and environmental risk assessment. *Sci. Total Environ.* 2014; 466:421–438.
15. Lolić A., Paíga P., Santos L.H., Ramos S., Correia M., Delerue-Matos C. Assessment of non-steroidal anti-inflammatory and analgesic pharmaceuticals in seawaters of North of Portugal: occurrence and environmental risk. *Sci. Total Environ.* 2015; 508:240–250.
16. Ferrari B.T., Paxéus N., Giudice R.L., Pollio A., Garric J. Ecotoxicological impact of pharmaceuticals found in treated wastewaters: study of carbamazepine, clofibric acid, and diclofenac. *Ecotoxicol. Environ. Saf.* 2003; 55(3):359–370.
17. Paul P.P., Kundu P., Karmakar U.K. Chemical and biological investigation of *Sanchezia nobilis* leaves extract. *Jordan J. Pharm. Sci.* 2022; 15(1):121–131.
18. Ternes T. Vorkommen von Pharmaka in Gewässern. *Wasser und Boden* 2001; 53(4):9–14.
19. Clara M., Strenn B., Ausserleitner M., Kreuzinger N. Comparison of the behaviour of selected micropollutants in a membrane bioreactor and a conventional wastewater treatment plant. *Water Sci. Technol.* 2004; 50(5):29–36.
20. Le T.K.N., Le N. Formulation and evaluation of herbal emulsion-based gel containing combined essential oils from *Melaleuca alternifolia* and *Citrus hystrix*. *Jordan J. Pharm. Sci.* 2024; 17(1):163–173.
21. Aziz K.H.H., Miessner H., Mueller S., Kalass D., Moeller D., Khorshid I., Rashid M.A.M. Degradation of pharmaceutical diclofenac and ibuprofen in aqueous solution, a direct comparison of ozonation, photocatalysis, and non-thermal plasma. *Chem. Eng. J.* 2017; 313:1033–1041.
22. Seifollahi Z., Rahbar-Kelishami A. Diclofenac extraction from aqueous solution by an emulsion liquid membrane: Parameter study and optimization using the response surface methodology. *J. Mol. Liq.* 2017; 231:1–10.
23. Yu H., Nie E., Xu J., Yan S., Cooper W.J., Song W. Degradation of diclofenac by advanced oxidation and reduction processes: kinetic studies, degradation pathways, and toxicity assessments. *Water Res.* 2013; 47(5):1909–1918.
24. Bae S., Kim D., Lee W. Degradation of diclofenac by pyrite catalyzed Fenton oxidation. *Appl. Catal. B Environ.* 2013; 134:93–102.
25. Viotti P.V., Moreira W.M., dos Santos O.A.A., Bergamasco R., Vieira A.M.S., Vieira M.F. Diclofenac removal from water by adsorption on Moringa oleifera pods and activated carbon: Mechanism, kinetic and equilibrium study. *J. Clean. Prod.* 2019; 219:809–817.
26. Carmalin Sophia A., Lima E.C., Allaudeen N., Rajan S. Application of graphene-based materials for adsorption of pharmaceutical traces from water and wastewater—a review. *Desalination Water Treat.* 2016; 57(57):27573–27586.

27. Poorsharbaf Ghavi F., Raouf F., Dadvand Koohi A. A review on diclofenac removal from aqueous solution, emphasizing on adsorption method. *Iran. J. Chem. Chem. Eng.* 2020; 39(1):141–154.
28. De Luna M.D.G., Budianta W., Rivera K.K.P., Arazo R.O. Removal of sodium diclofenac from aqueous solution by adsorbents derived from cocoa pod husks. *J. Environ. Chem. Eng.* 2017; 5(2):1465–1474.
29. dos Reis G.S., Bin Mahbub M.K., Wilhelm M., Lima E.C., Sampaio C.H., Saucier C., Pereira Dias S.L. Activated carbon from sewage sludge for removal of sodium diclofenac and nimesulide from aqueous solutions. *Korean J. Chem. Eng.* 2016; 33:3149–3161.
30. Nam S.-W., Jung C., Li H., Yu M., Flora J.R., Boateng L.K., Her N., Zoh K.-D., Yoon Y. Adsorption characteristics of diclofenac and sulfamethoxazole to graphene oxide in aqueous solution. *Chemosphere* 2015; 136:20–26.
31. Gil A., Santamaría L., Korili S. Removal of caffeine and diclofenac from aqueous solution by adsorption on multiwalled carbon nanotubes. *Colloid Interface Sci. Commun.* 2018; 22:25–28.
32. Maia G.S., de Andrade J.R., da Silva M.G., Vieira M.G. Adsorption of diclofenac sodium onto commercial organoclay: kinetic, equilibrium and thermodynamic study. *Powder Technol.* 2019; 345:140–150.
33. Malhotra M., Suresh S., Garg A. Tea waste derived activated carbon for the adsorption of sodium diclofenac from wastewater: adsorbent characteristics, adsorption isotherms, kinetics, and thermodynamics. *Environ. Sci. Pollut. Res.* 2018; 25:32210–32220.
34. Ministry of Agriculture, D. o. S. a. S. Annual Reports, Amman-Jordan, www.moa.gov.jo 2021.
35. Mahyoob W., Alakayleh Z., Hajar H.A.A., Al-Mawla L., Altwaiq A.M., Al-Remawi M., Al-Akayleh F. A novel co-processed olive tree leaves biomass for lead adsorption from contaminated water. *J. Contam. Hydrol.* 2022; 248:104025.
36. Yateem H., Afaneh I., Al-Rimawi F. Optimum conditions for oleuropein extraction from olive leaves. 2014.
37. Hamaidi M., Jaber N., Al-Remawi M., Elsayed A., Maghrabi I. A novel pharmaceutical excipient: Coprecipitation of calcium and magnesium silicate using brine-seawater in date palm cellulose as an absorbing host. *J. Excipients Food Chem.* 2017; 8(3).
38. Alakayleh Z., Al-Akayleh F., Al-Remawi M., Mahyoob W., Hajar H.A.A., Esaifan M., Shawabkeh R. Utilizing olive leaves biomass as an efficient adsorbent for ciprofloxacin removal: characterization, isotherm, kinetic, and thermodynamic analysis. *Environ. Monit. Assess.* 2024; 196(6):562.
39. Amoo K.O., Amoo T.E., Olafadehan O.A., Alagbe E.E., Adesina A.J., Bamigboye M.O., Olowookere B.D., Ajayi K.D. Adsorption of cobalt (II) ions from aqueous solution using cow bone and its derivatives: Kinetics, equilibrium and thermodynamic comparative studies. *Results Eng.* 2023; 20:101635.
40. Zhang W., Sheng X., Yan J., Wang J., Sun J., Zuo Q., Zhu X., Wang M., Gong L. The crucial role of different NaOH activation pathways on the algae-derived biochar toward carbamazepine adsorption. *Results Eng.* 2023; 20:101509.
41. Ghasemi M.R., Nazemi A.H., Bozorgzadeh H.R. Continuous adsorption process of CO2/N2/H2O from CH4 flow using type A zeolite adsorbents in the presence of ultrasonic waves. *Results Eng.* 2023; 20:101490.
42. De Almeida Ohana N., HM L.F., Luis N.-G. Adsorption of arsenic anions in water using modified lignocellulosic adsorbents. *Results Eng.* 2022; 13:100340.
43. Du X., Cui S., Fang X., Wang Q., Liu G. Adsorption of Cd (II), Cu (II), and Zn (II) by granules prepared using sludge from a drinking water purification plant. *J. Environ. Chem. Eng.* 2020; 8(6):104530.
44. Saimeh A.S., Alakayleh Z., Al-Akayleh F., Mahyoob W., Al-Remawi M., Abu Hajar H.A., Shawabkeh R., Ali Agha A.S. Chemically activated olive leaves biomass for efficient removal of methylene blue from contaminated aqueous solutions. *Emerg. Mater.* 2024; 1-15.

45. Cherik D., Louhab K. A kinetics, isotherms, and thermodynamic study of diclofenac adsorption using activated carbon prepared from olive stones. *J. Dispersion Sci. Technol.* 2018; 39(6):814-825.
46. Homagai P.L., Ghimire K.N., Inoue K. Adsorption behavior of heavy metals onto chemically modified sugarcane bagasse. *Bioresour. Technol.* 2010; 101(6):2067-2069.
47. Shirahama N., Moon S., Choi K.-H., Enjoji T., Kawano S., Korai Y., Tanoura M., Mochida I. Mechanistic study on adsorption and reduction of NO2 over activated carbon fibers. *Carbon* 2002; 40(14):2605-2611.
48. Bhutani P., Joshi G., Raja N., Bachhav N., Rajanna P.K., Bhutani H., Paul A.T., Kumar R. US FDA approved drugs from 2015–June 2020: a perspective. *J. Med. Chem.* 2021; 64(5):2339-2381.
49. Kaur M., Datta M. Adsorption characteristics of acid orange 10 from aqueous solutions onto montmorillonite clay. *Adsorption Sci. Technol.* 2011; 29(3):301-318.
50. Kaur M., Datta M. Diclofenac sodium adsorption onto montmorillonite: adsorption equilibrium studies and drug release kinetics. *Adsorption Sci. Technol.* 2014; 32(5):365-387.
51. Koopal L., Tan W., Avena M. Equilibrium mono-and multicomponent adsorption models: From homogeneous ideal to heterogeneous non-ideal binding. *Adv. Colloid Interface Sci.* 2020; 280:102138.
52. Park S.-H., Shin S.S., Park C.H., Jeon S., Gwon J., Lee S.-Y., Kim S.-J., Kim H.-J., Lee J.-H. Poly (acryloyl hydrazide)-grafted cellulose nanocrystal adsorbents with an excellent Cr (VI) adsorption capacity. *J. Hazard. Mater.* 2020; 394:122512.
53. Alakayleh Z. From inactive biomass in removing amoxicillin to new active chitosan-biomass composite adsorbents. *Results Eng.* 2025; 25:103709.
54. Tran H.N., Lima E.C., Juang R.-S., Bollinger J.-C., Chao H.-P. Thermodynamic parameters of liquid–phase adsorption process calculated from different equilibrium constants related to adsorption isotherms: A comparison study. *J. Environ. Chem. Eng.* 2021; 9(6):106674.
55. Alakayleh Z. Sulfuric acid-activated carbon from guava leaves for paracetamol adsorption. *Results Eng.* 2025; 25:103685.

امتزاز الديكلوفيناك من المياه الملوثة على مادة مازة مشتقة من أوراق الزيتون

زهير العكايلة [1]

[1] قسم الهندسة المدنية والبيئة، كلية الهندسة، جامعة مؤتة، مؤتة، الكرك، الأردن.

ملخص

تبحث هذه الدراسة في امتزاز الديكلوفيناك (DCF)على مادة مازة مشتقة من أوراق الزيتون. تم غسل أوراق الزيتون التي تم جمعها وتجفيفها وطحنها إلى مسحوق، ثم استخلاصها باستخدام الإيثانول (بنسبة نقاوة 80%). بعد ذلك، تم ترشيح المستخلص وغسله بهيبوكلوريت الصوديوم والإيثانول ثم تجفيفه. تم تنشيط المادة باستخدام هيدروكسيد الصوديوم وحمض الفوسفوريك ومياه البحر الميت لتعزيز قدرتها على امتزاز الديكلوفيناك من المياه الملوثة قيد الدراسة. تم دراسة تغيير عدة عوامل تشغيلية بشكل منهجي، مثل جرعة المادة المازة ووقت التلامس وتركيز الديكلوفيناك ودرجة الحموضة (pH)، لفهم تأثيرها على كفاءة الامتزاز. أظهرت دراسة حركية الامتزاز أن العملية تتبع نموذج حركية الامتزاز من المرتبة الثانية. كشفت دراسة إيزوثيرمات الامتزاز أن عملية الامتزاز تتبع نموذج فريندليش، مما يشير إلى حدوث امتزاز متعدد الطبقات على سطح غير متجانس. أظهرت الدراسة الثرموديناميكية للامتزاز أن عملية الامتزاز تلقائية وطاردة للحرارة. وأكد التحليل المورفولوجي باستخدام المجهر الإلكتروني الماسح (SEM)حدوث تغييرات في البنية المسامية للمادة المازة، مما يدل على الامتلاء الفعّال للمسام بجزيئات الديكلوفيناك بعد الامتزاز. بشكل عام، توضح النتائج فعالية المادة المازة المشتقة من أوراق الزيتون في إزالة الديكلوفيناك بكفاءة من المحاليل المائية.

الكلمات الدالة: التلوث؛ الملوثات الناشئة؛ الدراسة الثرموديناميكية؛ معالجة المياه؛ الامتزاز.

* ***المؤلف المراسل: زهير العكايلة***

zalakayleh@mutah.edu.jo

تاريخ استلام البحث 2024/05/13 وتاريخ قبوله للنشر 2024/07/18.